Cheng S *et al.* (2020)
Notulae Botanicae Horti Agrobotanici Cluj-Napoca 48(2):558-571
DOI:10.15835/nbha48211916
Research Article

Molecular responses of arbuscular mycorrhizal fungi in tolerating root rot of trifoliate orange

Shen CHENG[1], Li TIAN[1], Ying-Ning ZOU[1]*, Qiang-Sheng WU[1,2]*, Kamil KUČA[2], Popy BORA[3]

[1]*Yangtze University, College of Horticulture and Gardening, Jingzhou, Hubei 434025, China; 512760562@qq.com; 1943241801@qq.com; zouyingning@163.com (*corresponding author); wuqiangsh@163.com (*corresponding author)*
[2]*University of Hradec Kralove, Faculty of Science, Department of Chemistry, Hradec Kralove 50003, Czech Republic; kamil.kuca@uhk.cz*
[3]*Assam Agricultural University, Department of Plant Pathology, Jorhat, India; pbora.sonitpur10@gmail.com*

Abstract

Arbuscular mycorrhizal fungi (AMF) enhance plant disease resistance, while the underlying mechanisms in the molecular levels are not yet known. In this study, five-leaf-old trifoliate orange seedlings were inoculated with *Funneliformis mosseae* for 14 weeks and subsequently were infected by a citrus root rot pathogen *Phytophthora parasitica* by 7 days. The transcriptome results by Illumina HiSeq 4000 revealed that the percentage of Q30 bases reached 92.99% or above, and 29696 unigenes were annotated in a total of 63531 unigenes. 654 and 103 differentially expressed genes (DEGs) were respectively annotated in AMF-inoculated versus non-AMF-inoculated plants under non-infection and infection with *P. parasitica*, respectively, whilst these DEGs were related to defense mechanisms, signal transduction mechanisms and secondary metabolites biosynthesis. Forty-two genes were functionally annotated as the putative 'defense mechanism', whilst AMF inoculation induced 1 gene down-regulated and 3 genes up-regulated under *P. parasitica* infection. AMF inoculation stimulated more genes linked to signal transduction mechanism down-regulated than non-AMF plants. Eight genes were involved in secondary metabolites biosynthesis in AMF versus non-AMF seedlings under *P. parasitica*-infection conditions. Such transcriptome database provided total information in the molecular levels regarding mycorrhizal roles in tolerating *Phytophthora parasitica* infection.

Keywords: arbuscular mycorrhizal fungi; citrus; pathogen; RNA-Seq

Introduction

Citrus trees are susceptible to a large number of diseases, including root rot. The main pathogen of citrus root rot in China is *Phytophthora parasitica* (Tian *et al.*, 2018). Soil arbuscular mycorrhizal fungi (AMF) can build mutual symbionts with most plants (including citrus), viz. arbuscular mycorrhizas (AMs) (He *et al.*, 2019, 2020; Wu *et al.*, 2019; Zhang *et al.*, 2020). Many studies showed a crucial function of AMF on increased plant disease resistance (Xie *et al.*, 2019; Zhang *et al.*, 2019; Gao *et al.*, 2020). Ozgonen *et al.* (2010) inoculated AMF

Received: 05 May 2020. Received in revised form: 15 May 2020. Accepted: 21 May 2020. Published online: 30 Jun 2020.

on *Arachis hypogaea* plants to study its effects on stem rot caused by *Sclerotium rolfsii*, and found that all the selected AMF species, including *Funneliformis etunicatum*, *F. clarum*, *F. caledonium*, and *F. fasciculatum* collectively reduced the incidence of stem rot. Inoculation with *F. mosseae* and *Rhizophagus irregularis* also mitigated symptoms of root rot in *Aphanomyces euteiches*-infected pea (Bodker *et al*., 1998; Slezack *et al*., 1999). As a result, it seems that AMF has the capacity to mitigate root rot, whereas the underlying mechanisms are not yet known.

Transcriptome analysis with high-throughput sequencing (RNA-Seq), a new molecular biology technique, is designed to elucidate the molecular responses to bacteria-disease occurrence and fungi-disease occurrence (Gao *et al*., 2016). RNA-Seq technology also identifies responsive genes of pathogen infection from large-scale transcripts of plants, and further analyzes disease resistance mechanisms or pathogenic mechanisms through gene function analysis. Yap *et al*. (2005) found wound-induced proteins to activate the phosphorylation cascade in mycorrhiza-inoculated-*Medicago truncatula* by RNA-Seq. Dao *et al*. (2011) found a chalcone synthase from the transcriptome data of *M. truncatula* inoculated with *Glomus versiforme*, which could enhance plant disease resistance. Lambais and Mehdy (2010) found that in transcriptome of *Phaseolus vulgaris* plants, inoculation with *Rhizophagus irregularis* up-regulated chitinase and β-1,3-glucanase expression in differentially expressed genes (DEGs) to collectively hydrolyze cell walls of pathogenic fungi (Esquerré-Tugayé *et al*., 2000; Hu *et al*., 2017). These results conclude that RNA-Seq could reveal the potential mechanisms at the molecular level in disease resistance. However, information regarding AMF-enhanced resistance of root rot in molecular levels is scarce.

The objective of the present study was to establish the transcriptome of trifoliate orange (*Poncirus trifoliata* L. Raf.) roots after inoculated with an arbuscular mycorrhizal fungus *Funneliformis mosseae* and a citrus root rot pathogen *Phytophthora parasitica*, and to identify DEGs and their metabolic pathways after AMF inoculations.

Materials and Methods

Experimental design

The experiment consisted of a completely randomized block design with the inoculation with or without *Funneliformis mosseae* and the infection with or without *Phytophthora parasitica*. The four treatments were (i) the inoculation without *F. mosseae* and *P. parasitica* (*-F. m-P. p*), (ii) the inoculation with *F. mosseae* and without *P. parasitica* (*+F. m-P. p*), (iii) the inoculation with *P. parasitica* and without *F. mosseae (-F. m+P. p*), and (iv) the inoculation with *F. mosseae* and *P. parasitica* (*+F. m+P. p*). Each of four treatments was replicated five times.

Plant culture and pathogen inoculation

The arbuscular mycorrhizal fungal strain, *Funneliformis mosseae* (Nicol. & Gerd.) Schüßler & Walker [BGC XZ02A], was used in this study and also propagated with white clover in pots for 3 months, and mycorrhizal inoculums contained substrates, spores (20 spores/g), mycorrhizal hyphae, and infected root pieces.

Three 5-leaf-old trifoliate orange seedlings grown in autoclaved (0.11 MPa, 121 °C, 2h) sands were planted into 1.6-L plastic pots supplied with 1.5 kg of autoclaved substrates of soil and sand (5:1, v/v). At the same time, mycorrhizal inoculums (90 g per pot) of *F. mosseae* were applied into the rhizosphere of seedlings as the AMF treatment. In addition, an equal number of autoclaved mycorrhizal inoculums plus 2 mL filtrate (25 μm filter) of the inoculum were mixed with growth substrates as the non-AMF treatment. All the seedlings

were grown in a greenhouse for 14 weeks with 721 to 967 μmol/m^2/s photon flux, 25/19 °C average day/night temperature, and 75-85% relative humidity.

The pathogenic fungus *P. parasitica* was freely provided by the Citrus Research Institute, Chinese Academy of Agricultural Sciences. Such pathogenic infection was conducted out according to Li *et al*. (2014) with slight modification. Before the infection, the *P. parasitica* was cultured on potato dextrose agar (PDA) at 28 °C for one week. The 70% alcohol solution was utilized to sterilize the root neck of trifoliate orange seedlings for 10 s. After rinsed with sterilized water, a sterilized needle was used to make a wound, and 5-mm-diameter mycelial plug of *P. parasitica* was placed onto the wound. The non-*P. parasitica* infection treatment received sterilized PDA with same diameter. Subsequently, moistly sterilized absorbent cotton covered on the wound. After 7 days of the pathogen infection, the treated seedlings were harvested.

Illumina sequencing and data processing

The extraction of total RNA in the roots was done using an EASY spin Plus plant RNA kit (Aidlab Biotecnolohies CO. Ltd, China). DNAase (Takara Bio. Inc, Japan) was utilized to remove genomic DNA. After checked RNA yield, purity, and integrity, a total of the 12 RNA samples (three replicates (seedlings)/treatment) with 10 μg total RNA per replicate were sent for RNA-Seq by means of Illimina Genome Analyzer at Biomaker (Beijing, China) in 2017. After purified and concentrated polyadenylated mRNAs with dT-conjugated magnetic beads, directional RNA-Seq library was prepared. After reversed transcription from RNA to cDNA, PCR products with 200-500 bp were purified and quantified for sequencing. Whereafter, Illumina HiSeq 4000 platform was used to sequence the cDNA libraries of each treated root. The raw data were gathered by the sequencer. The raw sequence reads were uploaded into NCBI, in which the SRA number is SRR9665367.

The reads containing two N were eliminated, the adaptor was changed according to adapter information, and then the low-quality reads were trimmed to obtain clean data. Trinity software was used to assemble the clean data and acquire unigenes libraries of each sample.

Identification and annotation of DEGs

To identify DEGs, the edgeR software was utilized. Statistical significance indexes were established based on the fold change ($|\log_2 FC| \geq 2$) and p-value ($p \leq 0.01$). BLAST software (version 2.2.26) was used to compare DEGs with databases of COG, eggNOG4.5, GO, KOG, KEGG, NR, and Swiss-Prot to obtain annotation information. BLAST parameters e-value not greater than $1\times e^{-5}$ and HMMER parameters e-value not greater than $1\times e^{-10}$ were selected.

Results

Evaluation and splicing of sequencing data

A total of 85.80 Gb of clean data was obtained. The clean data of each samples reached 6.32 Gb, and the Q30 bases percentage was 93% or above (Table 1). As a result, the sequencing data in this study had good quality, which could meet the need for subsequent analysis. A total of 63531 unigenes were obtained by splicing, with a total length of 53714816 nt and N50 length of 1715 nt (Table 2). Among them, 15449 unigenes were longer than 1000 bp, and the average length of unigenes was 845.49 bp. In short, a high-quality transcriptome assembly database was obtained.

Table 1. Evaluation statistics of sample sequencing data

Samples	Read number	Base number	GC content	% ≥ Q30
-F. m-P. p 1	23134686	6914175344	44.13%	93.27%
-F. m-P. p 2	27933199	8338166762	43.77%	93.52%
-F. m-P. p 3	24333709	7266230434	43.98%	93.29%
-F. m+P. p 1	23036807	6885404058	43.83%	93.24%
-F. m+P. p 2	23153407	6927738352	43.66%	93.46%
-F. m+P. p 3	24267311	7262604330	43.42%	93.39%
+F. m-P. p 1	23614036	7063838768	43.99%	92.99%
+F. m-P. p 2	23095707	6901774502	43.84%	93.22%
+F. m-P. p 3	22801487	6813786472	44.37%	93.33%
+F. m+P. p 1	21160512	6321620442	43.93%	93.07%
+F. m+P. p 2	22483147	6719494016	43.81%	93.18%
+F. m+P. p 3	28074161	8387992504	43.78%	93.40%

Abbreviations: *+F. m*: inoculation with *Funneliformis mosseae*; *-F. m*: inoculation without *Funneliformis mosseae*; *+P. p*: infection with *Phytophthora parasitica*; *-P. p*: infection without *Phytophthora parasitica*.

Table 2. Statistics of assembly results

	Total number	Total length	Mean length	N50 length
Transcript	171478	287218347	1674.96	2617
Unigene	63531	53714816	845.49	1715

Screening of DEGs

Depending on the relative expression levels of the regulated samples, the DEGs were defined as up-regulated and down-regulated genes. Compared with *-F. m-P. p* treatment, *-F. m+P. p* treatment induced 99 genes up-regulated and 111 genes down-regulated in roots, while *+F. m-P. p* treatment induced 630 genes up-regulated and 662 genes down-regulated in roots (Table 3). Compared with *-F. m+P. p* treatment, *+F. m+P. p* treatment induced 36 genes up-regulated and 151 genes down-regulated in roots, and*+F. m-P. p* treatment modulated 665 genes up-regulated and 578 genes down-regulated.

Table 3. Differentially expressed gene numbers between different treated groups

Differential treatment groups	DEGs numbers	Up-regulated DEGs	Down-regulated DEGs
-F. m-P. p vs *-F. m+P. p*	210	99	111
-F. m-P. p vs *+F. m-P. p*	1292	630	662
-F. m+P. p vs *+F. m+P. p*	187	36	151
+F. m-P. p vs *+F. m+P. p*	1243	665	578

The abbreviations are the same as in Table 1.

GO functional enrichment of DEGs

GO terms were assigned to gain an overall understanding of the 110, 654, 103, and 623 DEGs identified in the *-F. m-P. p* vs *-F. m+P. p*, *-F. m-P. p* vs *+F. m-P. p*, *-F. m+P. p* vs *+F. m+P. p*, and *+F. m-P. p* vs *+F. m+P. p* analysis, respectively. The broad categories for the three major GO functional domains (biological process, cellular component, and molecular function) were shown (Figure 1). Compared with *-F. m-P. p* treatment, *-F. m+P. p* treatment induced a total of 110 DEGs annotated to the secondary node of GO database (Figure 1a). In the biological process, "biological regulation", "cellular process", "localization", "metabolic process", "response to stimulus", and "single-organism process" captured 22 (25%), 58 (53%), 22 (25%), 68 (62%), 33 (30%) and 57 (52%) unigenes, respectively. In the cellular components, "cell", "cell part", "membrane", and "organelle" annotated captured 41 (37%), 23 (21%), and 25 (23%) unigenes, respectively. In the molecular

function, "catalytic activity", "binding", and "transporter activity" captured 75 (68%), 51 (46%), and 13 (12%) unigenes, respectively.

Compared with *-F. m-P. p* treatment, *+F. m-P. p* treatment induced a total of 654 DEGs annotated to the secondary node of GO database (Figure 1b). In the biological process, "metabolic process", "single-organism process", "cellular process", "response to stimulus", and "biological regulation" captured 369 (56%), 292 (45%), 277 (42%), 156 (24%) and 126 (19%) unigenes, respectively. In the cellular component, "cell" (205, 31%), "cell part" (205, 31%), "membrane" (163, 25%), and "organelle" (127, 19%) captured most of the annotated unigenes. In the molecular function, "catalytic activity" (395, 60%), "binding" (295, 45%), and "transporter activity" (67, 10%) captured most of the annotated unigenes.

Compared with *-F. m+P. p* treatment, *+F. m+P. p* treatment induced a total of 103 DEGs annotated to the secondary node of GO database (Figure 1c). In the biological process, "biological regulation" (21, 20%), "cellular process" (53, 48%), "localization" (19, 18%), "metabolic process" (57, 55%), "response to stimulus" (30, 29%), and "single-organism process" (41, 40%) captured most of the annotated unigenes; In the cellular component, "cell" (42, 41%), "cell part" (42, 41%), "membrane" (30, 29%), and "organelle" (25, 24%) captured most of the annotated unigenes. In the molecular function, only "catalytic activity" (57, 55%) and "binding" (54, 52%) captured most of the annotated unigenes.

Compared with *+F. m-P. p* treatment, *+F. m+P. p* treatment induced a total of 623 DEGs annotated to the secondary node of GO database (Figure 1d). In the biological process, "metabolic process" (337, 54%), "single-organism process" (274, 44%), "cellular process" (255, 41%), "response to stimulus" (157, 25%), "biological regulation" (112, 18%), and "localization" (99, 16%) captured most of the annotated unigenes. In the cellular component, "cell" (186, 30%), "cell part" (186, 30%), "membrane" (139, 22%), and "organelle" (117, 19%) captured most of the annotated unigenes. In the molecular function, only "catalytic activity" (371, 60%) and "binding" (267, 43%) captured most of the annotated unigenes.

COG classification of DEGs

Compared with *-F. m-P. p* treatment, *-F. m+P.* p treatment induced a total of 80 DEGs annotated to 19 COG classifications (Figure 2a). Among the 19 COG classifications, "general function prediction" catched most of the DEGs (18, 23%), followed by "transcription" (11, 14%). Besides, "replication, recombination and repair", "posttranslational modification, protein turnover, chaperones", and "carbohydrate transport and metabolism" all catched 10 DEGs. In addition, 9 DEGs were captured by "secondary metabolites biosynthesis, transport and catabolism", indicating that these genes may be involved in the secondary metabolites biosynthesis of citrus. Additionally, 5 DEGs and 7 DEGs were annotated respectively to "signal transduction mechanisms" and "defense mechanisms", suggesting that these genes may play a role in resisting pathogen infection.

The *+F. m-P. p* treatment induced a total of 403 DEGs annotated to 22 COG classifications, relative to *-F. m-P. p* treatment (Figure 2b). Among the 22 COG classifications, "general function prediction" caught most of the DEGs (125, 31%), followed by "signal transduction mechanisms" (66, 16%), "transcription" (63, 16%), and "replication, recombination and repair" (60, 15%). Whereas, "secondary metabolites biosynthesis, transport and catabolism" and "defense mechanisms" captured 48 and 19 DEGs respectively, implying that these genes may participate in plant resistance enhancement induced by AMF.

Compared with *-F. m+P. p* treatment, *+F. m+P. p* treatment induced a total of 53 DEGs annotated to 18 COG classifications (Figure 2c). Among the 18 COG classifications, "general function prediction" caught most of the DEGs (15, 28%), followed by "transcription" (7, 13%) and "signal transduction mechanisms" (7, 13%). In addition, "secondary metabolites biosynthesis, transport and catabolism" and "defense mechanisms" captured 4 DEGs, showing that these genes took part in plant resistance enhancement induced by AMF.

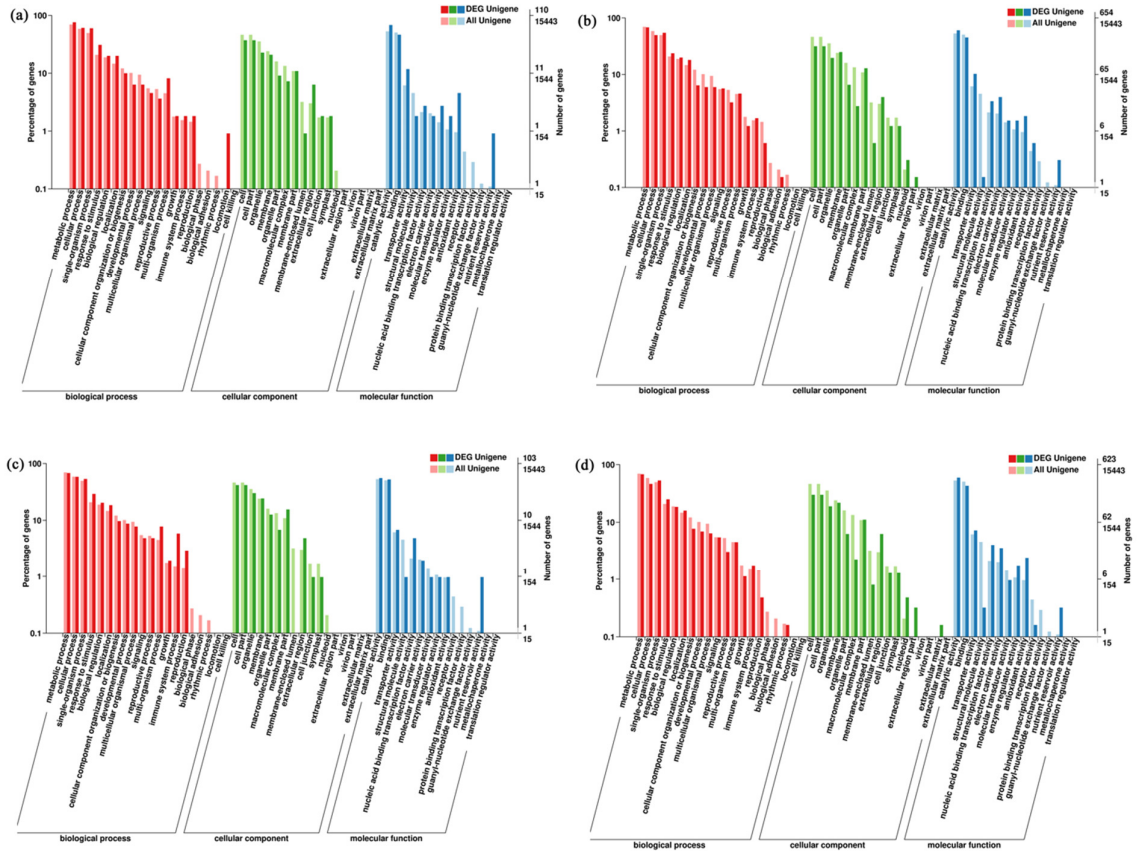

Figure 1. Gene ontology classifications of differentially expressed genes between *-F. m-P. p* and *-F. m+P. p* (a), *-F. m-P. p* and *+F. m-P. p* (b), *-F. m+P. p* and *+F. m+P. p* (c), and *+F. m-P. p* and *+F. m+P. p* (d), respectively. The abbreviations are the same as in Table 1

Compared with *+F. m-P. p* treatment, *+F. m+P. p* treatment induced a total of 346 DEGs annotated to 22 COG classifications (Figure 2d). Among the 22 COG classifications, "general function prediction" caught most of the DEGs (104, 30%), followed by "transcription" (51, 15%), "signal transduction mechanisms" (50, 14%), and "replication, recombination and repair" (46, 13%). Moreover, 40 DEGs and 14 DEGs were annotated respectively to "secondary metabolites biosynthesis, transport and catabolism" and "defense mechanisms", and these genes may uncover the defense mechanisms induced by AMF when plants were suffered from the pathogen infection.

Root DEGs related to defense mechanism

After blasted with a serial of databases, there were 42 unigenes functionally annotated as the putative "defense mechanism" of all differential treated groups in at least one database (Table 4). Compared with non-mycorrhizal plants, mycorrhizal plants induced 24 unigenes down-regulated and 3 unigenes up-regulated under the condition of no pathogen infection. The biggest drop was c42319.graph_c0 (-6.85) and the biggest rise was c44347.graph_c0 (1.59). Compared with non-mycorrhizal plants, mycorrhizal plants induced 1 unigene (c41443.graph_c0, -3.51) down-regulated and 3 unigenes up-regulated in the presence of the pathogen infection, whilst the biggest rise was c46155.graph_c0 (1.92). Additionally, *P. parasitica* infection induced 4 unigenes down-regulated and 19 unigenes up-regulated than non-*P. parasitica* infection treatment in mycorrhizal seedlings. In non-mycorrhizal seedlings, *P. parasitica* infection induced 8 unigenes down-regulated

and 1 unigene up-regulated, indicating that mycorrhizal seedlings performed more actively than non-mycorrhizal seedlings to response to *P. parasitica* infection.

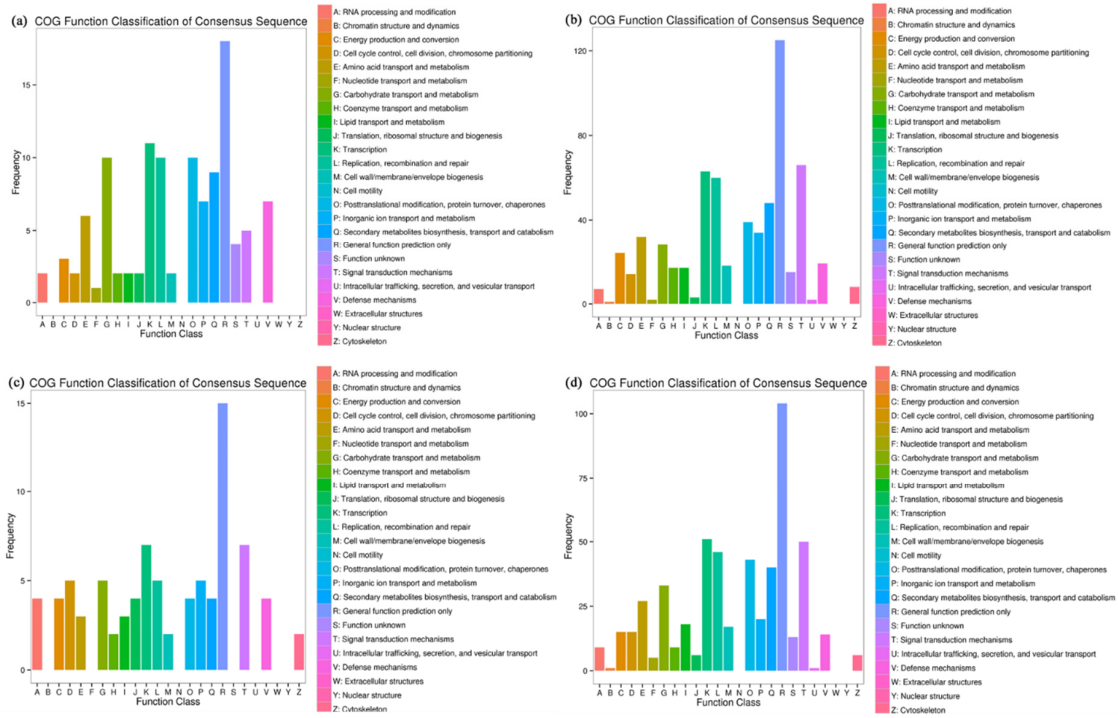

Figure 2. COG functional classification of differentially expressed genes between *-F. m-P. p* and *-F. m+P. p* (a), *-F. m-P. p* and *+F. m-P. p* (b), *-F. m+P. p* and *+F. m+P. p* (c), and *+F. m-P. p* and *+F. m+P. p* (d), respectively. The abbreviations are the same as in Table 1

Root DEGs related to signal transduction mechanism

After blasted with a serial of databases, lots of unigenes functionally annotated as the putative "signal transduction mechanism" of all differential treatment groups in at least one database, and the top 10 unigenes with the highest expression in each difference treatment group was selected for analysis. The blast results of the 40 unigenes in the Orange Genome Annotation Project database were shown in Table 5. The 40 unigenes were mostly annotated as calcium-binding protein, protein serine/threonine kinase, phosphoinositol kinase, and leucine-rich repeat receptor protein kinase, which were acted as the mediators of signal transmission and play a role in the middle and downstream of signal transduction in the Orange Genome Annotation Project database. In the *-F. m-P. p* vs *-F. m+P. p* group, there were 6 unigenes up-regulated and 4 unigenes down-regulated in the first 10 expression levels. The most significantly up-regulated gene was c48447.graph_c0 by 1.7 times, and the most significantly down-regulated gene was c43034.graph_c0 by 4.3 times. The annotation information of c47577.graph_c1 and c41969.graph_c1 in the sweet orange database was WRKY19 and MAPK3, respectively, and the expressions of the two genes were collectively down-regulated. In the *-F. m-P. p* vs *+F. m-P. p* group, the unigenes in the top 10 expressions were up-regulated for 3 unigenes and down-regulated for 7 unigenes. The most significant up-regulation was c48165.graph_c0, up by 3.44 times, and its annotation information in the sweet orange database was WRKY46.

Table 4. Forty-two DEGs related to defense mechanisms

No.	Gene ID	*-F. m-P. p* vs *-F. m+P. p*	*-F. m-P. p* vs *+F. m-P. p*	*-F. m+P. p* vs *+F. m+P. p*	*+F. m-P. p* vs *+F. m+P. p*	Gene ID in *Citrus sinensis*	*Citrus sinensis* annotation results
1	c17504.graph_c0	-1.02	--	--	--	Cs1g13660	Pleiotropic drug resistance protein 1; ABC transporter G family member 40
2	c45869.graph_c0	-4.73	-5.92	--	2.03	Cs5g13760	Pleiotropic drug resistance protein 3; ABC transporter G family member 37
3	c35922.graph_c0	-2.17	-2.91	--	--	Cs5g10270	Multidrug and toxin extrusion protein 1
4	c43566.graph_c0	-1.21	--	--	--	Cs4g17100	ABC transporter G family member 32; Pleiotropic drug resistance protein 6
5	c42319.graph_c0	-4.44	-6.85	--	--	Cs2g07290	NADPH-dependent methylglyoxal reductase GRE2
6	c44774.graph_c0	1.88	--	--	2.04	Cs3g14510	Probable carboxylesterase 15
7	c48128.graph_c3	-1.23	--	1.30	--	Cs1g15710	ABC transporter G family member 36; Pleiotropic drug resistance protein12
8	c46744.graph_c2	-1.15	--	1.21	--	Cs7g32530	Probable multidrug resistance-associated protein lethal(2)03659
9	c40817.graph_c0	-1.92	-1.79	--	--	Cs7g01770	MATE efflux family protein FRD3
10	c41832.graph_c0	--	-1.62	--	1.71	Cs7g19610	E3 ubiquitin-protein ligase ORTHRUS 2
11	c30352.graph_c0	--	-1.74	--	2.04	Cs3g13090	NADPH-dependent aldehyde reductase ARI1
12	c23405.graph_c0	--	-1.03	--	--	Cs6g19470	ABC transporter G family member 14
13	c46884.graph_c0	--	-1.01	--	--	Cs5g19190	Probable carboxylesterase 18;Hormone-sensitive lipase
14	c46035.graph_c0	--	1.20	--	--	Cs9g13790	Histone-lysine N-methyltransferase, H3 lysine-9 specific SUVH5
15	c40353.graph_c0	--	-2.79	--	3.27	Cs8g09790	Bifunctional dihydroflavonol 4-reductase/flavanone 4-reductase
16	c23693.graph_c0	--	-1.00	--	--	Cs9g06490	Probable carboxylesterase 12
17	c48015.graph_c0	--	1.05	--	--	Cs1g26350	MATE efflux family protein 3, chloroplastic
18	c32593.graph_c0	--	-1.57	--	1.75	--	--
19	c31739.graph_c0	--	-1.64	--	1.71	Cs1g18930	Pleiotropic drug resistance protein 1; ABC transporter G family member 40
20	c45483.graph_c0	--	-1.02	--	--	Cs5g19630	Multidrug and toxin extrusion protein 1
21	c44347.graph_c0	--	1.59	--	--	Cs7g12620	MATE efflux family protein 7
22	c17070.graph_c0	--	-2.04	--	2.08	Cs1g13730	Pleiotropic drug resistance protein 1; ABC transporter G family member 4
23	c41443.graph_c0	--	-6.42	-3.51	3.06	Cs9g11040	Multidrug resistance protein 1;ABC transporter B family member 19
24	c39782.graph_c1	--	-2.39	--	--	Cs2g20580	Probable tyrosine-protein phosphatase At1g05000
25	c39825.graph_c0	--	-1.61	--	--	Cs9g06450	Probable carboxylesterase 2
26	c31917.graph_c0	--	-1.45	--	1.47	Cs9g01170	Multidrug resistance protein homolog 49

27	c47660.graph_c0	--	-2.49	--	1.60	Cs7g10200	Multidrug resistance-associated protein 2, 6 (Mrp2, 6), abc-transoprter
28	c17070.graph_c1	--	-2.09	--	2.62	Cs1g13730	Pleiotropic drug resistance protein 1; ABC transporter G family member 4
29	c48327.graph_c1	--	-1.43	--	--	Cs6g02250	Pleiotropic drug resistance protein 3; ABC transporter G family member 37
30	c42651.graph_c0	--	-3.25	--	1.47	Cs4g11230	Putative multidrug resistance protein; ABC transporter B family member 15
31	c35526.graph_c0	--	-2.92	--	--	Cs4g20440	Putative pleiotropic drug resistance protein 7
32	c41867.graph_c0	--	-1.20	--	--	Cs4g09600	Lipid-binding serum glycoprotein family protein
33	c46155.graph_c0	--	--	1.92	1.79	orange1.1t00127	Pleiotropic drug resistance protein 1
34	c33501.graph_c0	--	--	--	-1.11	Cs2g21180	B-cell receptor-associated protein 31-like containing protein, expressed
35	c40502.graph_c1	--	--	--	-1.74	orange1.1t02755	Putative NADPH-dependent methylglyoxal reductase GRP2
36	c38995.graph_c0	--	--	--	-1.20	Cs2g28050	Dual specificity phosphatase, catalytic domain containing protein, expressed
37	c31723.graph_c0	--	--	--	-1.84	Cs6g13330	ABC transporter G family member 22;Pleiotropic drug resistance protein 3
38	c30019.graph_c0	--	--	--	1.01	Cs6g15300	Pleiotropic drug resistance protein 2
39	c24119.graph_c0	--	--	--	1.72	--	--
40	c48446.graph_c0	--	--	--	1.92	Cs6g20280	ABC transporter B family member 15; Putative multidrug resistance protein
41	c42131.graph_c0	--	--	--	2.70	Cs8g05610	Probable carboxylesterase 13
42	c42785.graph_c0	--	--	--	2.64	Cs1g16850	Multidrug resistance protein homolog 65

The most significant down-regulation was c49730.graph_c0, down by 7.98 times. In the *-F. m+P. p* vs *+F. m+P. p* group, the unigenes in the top 10 expressions were up-regulated for 2 unigenes and down-regulated for 8 unigenes. The up-regulated genes were c48593.graph_c1 (1.34) and c44707.graph_c0 (1.29). Among the down-regulated genes, the most significant one was c49730.graph_c0, which was down-regulated by 8.19 times. In the *+F. m-P. p* vs *+F. m+P. p* group, the unigenes in the top 10 expressions were up-regulated for 8 genes and down-regulated for 2 genes. The most significant up-regulation was c35123.graph_c0 increased by 5.02 times. The most significant down-regulation was c28686.graph_c0 decreased by 3.16 times. Interestingly, whether trifoliate orange seedlings were infected by the pathogen or not, mycorrhizal plants induced more down-regulated genes than non-mycorrhizal plants.

Root DEGs related to secondary metabolites biosynthesis

After blasted, lots of unigenes were functionally annotated to the putative "secondary metabolites biosynthesis" of all different treatment groups in at least one database, whilst the top 10 unigenes with the highest expression in each different treatment group was selected for analysis. The blast results regarding the 38 unigenes in the Orange Genome Annotation Project database were shown in Table 6.

Table 5. Forty DEGs linked to signal transduction mechanisms

No.	Gene ID	Expression situation	Gene ID in *Citrus sinensis*	*Citrus sinensis* annotation results
1	c43034.graph_c0	-4.30	Cs9g10150	Putative protein phosphatase 2C-like protein 44
2	c47577.graph_c1	-2.54	Cs5g22460	Probable WRKY transcription factor 19
3	c41969.graph_c1	-2.07	orange1.1t03917	Mitogen-activated protein kinase kinase kinase 3
4	c48447.graph_c0	1.70	Cs6g06700	Probable LRR receptor-like serine/threonine-protein kinase At1g56140
5	c48566.graph_c1	-1.61	orange1.1t01898	Putative disease resistance protein RGA3; Putative inactive disease susceptibility protein LOV1
6	c43651.graph_c0	1.48	Cs6g11630	Probable receptor-like protein kinase At5g18500;Proline-rich receptor-like protein kinase PERK5
7	c33248.graph_c1	1.27	Cs2g27050	Copine (Calcium-dependent phospholipid-binding protein) family protein
8	c45715.graph_c1	1.13	Cs5g02190	Pleckstrin homology (PH) domain-containing protein
9	c44894.graph_c0	1.04	--	--
10	c48333.graph_c3	1.04	Cs7g25380	Putative uncharacterized protein Sb02g028510
11	c49730.graph_c0	-7.98	--	--
12	c28017.graph_c1	-4.15	Cs9g12300	Wall-associated receptor kinase-like 22
13	c35123.graph_c0	-3.58	orange1.1t01650	Probable inositol polyphosphate 5-phosphatase C9G1.10c
14	c29587.graph_c0	-3.57	Cs8g12690	Calcium-dependent protein kinase 33
15	c41501.graph_c0	-3.56	Cs1g16130	Probable LRR receptor-like serine/threonine-protein kinase At1g05700
16	c43034.graph_c0	-3.50	Cs9g10150	Putative protein phosphatase 2C-like protein 44
17	c48165.graph_c0	3.44	orange1.1t00472	Probable WRKY transcription factor 46
18	c28017.graph_c0	-3.12	orange1.1t03406	Probable LRR receptor-like serine/threonine-protein kinase At5g48740
19	c47598.graph_c1	2.58	Cs7g16030	Disease resistance protein RGA2
20	c28686.graph_c0	2.42	Cs5g07160	Calcium-binding protein CML38
21	c49730.graph_c0	-8.19	--	--
22	c45469.graph_c0	-1.85	Cs3g02640	Leucine-rich repeat receptor-like protein kinase (Fragment)
23	c29997.graph_c0	-1.64	Cs6g21420	Calcium-binding protein CML42
24	c46150.graph_c0	-1.61	Cs6g17410	Diphosphoinositol polyphosphate phosphohydrolase 1
25	c46512.graph_c0	-1.56	Cs8g20420	Probable protein phosphatase 2C 25
26	c39683.graph_c0	-1.38	Cs2g17370	Diphosphoinositol polyphosphate phosphohydrolase, putative
27	c48593.graph_c1	1.34	Cs5g21040	Disease resistance protein RGA2
28	c44707.graph_c0	1.29	Cs8g20580	Probable LRR receptor-like serine/threonine-protein kinase MRH1
29	c44894.graph_c0	-1.27	--	--
30	c16791.graph_c0	-1.22	orange1.1t04033	Protein belonging to uncharacterized protein family UPF0047
31	c35123.graph_c0	5.02	orange1.1t01650	Probable inositol polyphosphate 5-phosphatase C9G1.10c
32	c34446.graph_c1	4.74	Cs3g26960	Neutral/alkaline nonlysosomal ceramidase family protein
33	c34446.graph_c0	4.45	Cs3g26960	Neutral/alkaline nonlysosomal ceramidase family protein
34	c25753.graph_c0	3.33	Cs1g13850	Putative uncharacterized protein Sb01g021605 (Fragment)
35	c28017.graph_c1	3.19	orange1.1t03406	Probable LRR receptor-like serine/threonine-protein kinase At5g48740
36	c28686.graph_c0	-3.16	Cs5g07160	Calcium-binding protein CML38
37	c39912.graph_c0	2.98	Cs3g16870	Oligopeptide transporter 4
38	c41501.graph_c0	2.86	Cs1g16130	Probable LRR receptor-like serine/threonine-protein kinase At1g05700
39	c47598.graph_c1	-2.71	Cs7g16030	Disease resistance protein RGA2
40	c46653.graph_c0	2.61	Cs1g26020	Probable LRR receptor-like serine/threonine-protein kinase At1g51880

1-10:*-F. m-P. p* vs *-F. m+P. p*; 11-20:*-F. m-P. p* vs *+F. m-P. p*; 21-30:*-F. m+P. p* vs *+F. m+P. p*; 31-40:*+F. m-P. p* vs *+F. m+P. p*. The abbreviations are the same as in Table 1.

In the *-F. m-P. p* vs *-F. m+P. p* group, there were one gene (c43852.graph_c0, 1.12) up-regulated and nine genes down-regulated in the unigenes according to the top 10 expression levels. The most significant down-regulation was c29552.graph_c0, down by 5.72 times. In the *-F. m-P. p* vs *+F. m-P. p* group, the unigenes in the top 10 expression levels all presented down-regulation pattern, and the most significant down-regulation was c29552.graph_c0, down by 7.29 times. In the *-F. m+P. p* vs *+F. m+P. p* group, only 8 unigenes showed

differential expression pattern, among which 5 genes were up-regulated and 3 genes were down-regulated. The most significant up-regulation was c41941.graph_c0 increased by 2.1 times. The most significant down-regulation was c41443.graph_c0 decreased by 3.51 times. In the *+F. m-P. p* vs *+F. m+P. p* group, the unigenes in the top 10 expression levels all presented up-regulation pattern, whilst the most significant up-regulation was c41443.graph_c0 increased by 4.73 times.

Table 6. 38 DEGs related to secondary metabolites biosynthesis

No.	DEGs	Expression sitiation	*Citrus sinensis*	*Citrus sinensis* annotation results
1	c29552.graph_c0	-5.72	Cs4g12540	Flavonol synthase/flavanone 3-hydroxylase; 1-aminocyclopropane-1-carboxylate oxidase homolog 11
2	c40823.graph_c0	-5.40	Cs3g24170	Flavonoid 3'-monooxygenase
3	c45869.graph_c0	-4.73	Cs5g13760	Pleiotropic drug resistance protein 3; ABC transporter G family member 37
4	c42319.graph_c0	-4.44	Cs2g07290	NADPH-dependent methylglyoxal reductase GRE2
5	c48120.graph_c0	-1.90	orange1.1t00399	Ferric reduction oxidase 2;NADPH oxidase 1
6	c45773.graph_c0	-1.74	Cs9g05770	1,4-beta-D-glucanase;
7	c48128.graph_c3	-1.23	Cs1g15710	Pleiotropic drug resistance protein 12
8	c43566.graph_c0	-1.21	Cs4g17100	ABC transporter G family member 32; Pleiotropic drug resistance protein 6
9	c46744.graph_c2	-1.15	Cs7g32530	Multidrug resistance-associated protein 1
10	c43852.graph_c0	1.12	Cs2g30870	Saccharopine dehydrogenase family protein, expressed
11	c29552.graph_c0	-7.29	Cs4g12540	Flavonol synthase/flavanone 3-hydroxylase; 1-aminocyclopropane-1-carboxylate oxidase homolog 11
12	c42319.graph_c0	-6.85	Cs2g07290	NADPH-dependent methylglyoxal reductase GRE2
13	c40823.graph_c0	-6.57	Cs3g24170	Flavonoid 3'-monooxygenase
14	c41443.graph_c0	-6.42	Cs9g11040	Multidrug resistance protein 1
15	c45869.graph_c0	-5.92	Cs5g13760	Pleiotropic drug resistance protein 3; ABC transporter G family member 37
16	c40233.graph_c0	-5.03	Cs6g15620	Flavonoid 3'-monooxygenase;Probable (S)-N-methylcoclaurine 3'-hydroxylase isozyme 2
17	c48217.graph_c0	-3.93	Cs4g19530	Carotenoid 9,10(9',10')-cleavage dioxygenase 1
18	c47071.graph_c0	-3.80	Cs7g31750	Flavone synthase; Flavanone 3-dioxygenase
19	c22631.graph_c0	-3.47	orange1.1t01744	Bacilysin biosynthesis oxidoreductase BacC
20	c42651.graph_c0	-3.25	Cs4g11230	Multidrug resistance protein 1
21	c41443.graph_c0	-3.51	Cs9g11040	Multidrug resistance protein 1
22	c40233.graph_c0	-2.89	Cs6g15620	Flavonoid 3'-monooxygenase;Probable (S)-N-methylcoclaurine 3'-hydroxylase isozyme 2
23	c47071.graph_c0	-2.72	Cs7g31750	Flavone synthase; Flavanone 3-dioxygenase
24	c41941.graph_c0	2.10	Cs5g28750	Flavonol synthase/flavanone 3-hydroxylase
25	c46155.graph_c0	1.92	orange1.1t00127	Pleiotropic drug resistance protein 1
26	c42229.graph_c1	1.91	Cs7g23790	Polyamine oxidase
27	c48128.graph_c3	1.30	Cs1g15710	Pleiotropic drug resistance protein 12
28	c46744.graph_c2	1.21	Cs7g32530	Multidrug resistance-associated protein 1
29	c23556.graph_c1	4.73	Cs3g21210	Abscisic acid 8'-hydroxylase 3; 3-epi-6-deoxocathasterone 23-monooxygenase
30	c46582.graph_c0	3.78	Cs1g23100	L-ascorbate oxidase homolog
31	c41962.graph_c0	3.56	Cs2g03380	Flavonol synthase/flavanone 3-hydroxylase;Probable 1-aminocyclopropane-1-carboxylate oxidase
32	c36650.graph_c3	3.51	Cs6g07450	Laccase-7; Laccase-9; Laccase-8; Laccase-12; Laccase-24; Laccase-3; Laccase-14
33	c41443.graph_c0	3.06	Cs9g11040	Multidrug resistance protein 1
34	c29897.graph_c0	3.02	orange1.1t05246	Immunoglobulin/major histocompatibility complex
35	c22631.graph_c0	2.86	orange1.1t01744	Momilactone A synthase;Glucose 1-dehydrogenase B
36	c42785.graph_c0	2.64	Cs1g16850	Multidrug resistance protein 1;Multidrug resistance protein homolog 65
37	c17070.graph_c1	2.62	Cs1g13730	Pleiotropic drug resistance protein 1; ABC transporter G family member 40
38	c49268.graph_c0	2.55	Cs4g20350	Gibberellin 3-beta-dioxygenase 1;Flavone synthase; Flavonol synthase/flavanone 3-hydroxylase

1-10: *-F. m-P. p* vs *-F. m+P. p*; 11-20:*-F. m-P. p* vs *+F. m-P. p*; 21-28:*-F. m+P. p* vs *+F. m+P. p*; 29-38:*+F. m-P. p* vs *+F. m+P. p*. The abbreviations are the same as in Table 1

Discussion

The construction of gene expression profiles through transcriptome sequencing is an important approach for non-model plants lacking genomic sequence data. Lambais and Mehdy (2010) screened out chitinase- and β-1,3-glucanase-related DEGs from the transcripts of *Phaseolus vulgaris* inoculated with *Rhizophagus irregularis*. Chitinase and β-1,3-glucanase, as important secondary metabolites in plants, inhibit the infection of pathogenic fungi and improve the disease resistance of plants (Ebrahim *et al*., 2011). Ward and Weber (2012) used RNA-Seq technology to sequence the resistant strains of raspberry 'Latham' infected by root rot pathogen (*Phytophthora rubi*), and found that pathogenesis-related protein genes, as well as genes related to tricarboxylic acid cycle and lignin synthesis pathway all presented up-regulation. Cicatelli *et al*. (2012) and Vangelisti *et al*. (2018) also demonstrated the positive effects of secondary metabolites induced by AMF in tolerating abiotic stress through RNA-Seq technology. In this work, DEGs related to secondary metabolites biosynthesis presented up-regulation in mycorrhizal plants when suffered the pathogen infection, while DEGs related to secondary metabolites biosynthesis presented down-regulation in non-mycorrhizal plants when suffered the pathogen infection. This indicated that mycorrhizal plants can actively induce the up-regulated expression of the genes related to secondary metabolites biosynthesis to respond to the pathogen infection.

Signal transduction is a key link in plant response to external stimulus (Kaur and Gupta, 2005). In this work, compared with *-F. m-P. p* vs *-F. m+P. p*, the number and expression level of DEGs annotated as receptor-like protein kinases (RLKs) in *+F. m-P. p* vs *+F. m+P. p* differential gene set were more and higher. This kind of protein kinase is a transmembrane protein kinase located on the plasma membrane surface, which can be activated in large quantities under the action of various stress factors, and participate in the signal transduction process to induce plant disease resistance (Xu *et al*., 2002). In our work, the expression of gene that annotated as mitogen-activated protein kinase kinase kinase 3 in *-F. m-P. p* vs *-F. m+P. p* differential gene set was down-regulated by 2.07 times, which was in accordance with the result of Liu *et al*. (2017) in mango after infected by *Fusarium mangiferae*. However, compared with *-F. m-P. p* vs *-F. m+P. p* differential treatment group, DEGs in *+F. m-P. p* vs *+F. m+P. p* were more up-regulated, suggesting that mycorrhizal plants can regulate the up-regulated expression of more genes related to signal transduction to respond to the pathogen infection. However, mycorrhizal inoculation induced the top 10 DEGs related to signal transduction assumed down-regulation of 8 genes and up-regulation of 2 genes when suffered the pathogen infection in comparison with non-mycorrhizal treatment. This might be because mycorrhizal plants selectively mobilize related signal transduction pathways, which needs to be further studied.

Many of the DEGs were linked to cell physiological processes, metabolic processes, stimulus response, catalytic activity, and transcriptional activity in the GO secondary node. Moreover, expression of more genes was induced by AMF inoculation in non-pathogen-infected plants than in pathogen-infected plants. However, from the number of DEGs between *-F. m-P. p* vs *-F. m+P. p* and *+F. m-P. p* vs *+F. m+P. p*, it found that mycorrhizal plants induced more gene expression than non-mycorrhizal plants when suffered *P. parasitica* infection. It suggests that although the pathogen infection significantly inhibited the positive effect of AMF inoculation in plants, mycorrhizal plants still regulate various defense mechanisms inside plants to respond to the pathogen infection. In addition, the expression situation of DEGs in secondary metabolites biosynthesis, signal transduction mechanism and defense mechanism in the COG database in the four differentially treatment groups were similar to that in GO secondary node. This further illustrates the important role of AMF inoculation in the response of *P. parasitica* infection. The annotation results of DEGs in each functional classification of each treatment group also provided important information and data for digging the key genes associated with the defense mechanism of trifoliate orange after AMF inoculation. All these unigenes may become the important information resource for future genetic research in mycorrhizal roles in enhancing tolerance of trifoliate orange in response to biotic stress.

Acknowledgements

This study was supported by the Scientific and Technological Innovation Team of Outstanding Youth Scientist, Hubei Provincial Department of Education (T201604).

Conflict of Interests

The authors declare that there are no conflicts of interest related to this article.

References

Bodker L, Kjoller R, Rosendahl S (1998). Effect of phosphate and the arbuscular mycorrhizal fungus *Glomus intraradices* on disease severity of root rot of peas (*Pisum sativum*) caused by Aphanomyces euteiches. Mycorrhiza 8:169-174.

Cicatelli A, Lingua G, Todeschini V, Biondi S, Torrigiani P, Castiglione S (2012). Arbuscular mycorrhizal fungi modulate the leaf transcriptome of a populus alba l. clone grown on a zinc and copper-contaminated soil. Environmental and Experimental Botany 75:25-35.

Dao TT, Linthorst HJ, Verpoort R (2011). Chalcone synthase and its functions in plant resistance. Phytochemistry Reviews 10:397-412.

Ebrahim S, Usha K, Singh B (2011). Pathogeneisi-related (PR)-proteins: Chinase and β-1,3-glucanase in defense mechanism against malformation in mango (*Mangifera indica* L.). Scientia Horticulturae 130:847-852.

Esquerré-Tugayé MT, Boudart G, Dumas B (2000). Cell wall degrading enzymes, inhibitory proteins, and oligosaccharides participate in the molecular dialogue between plants and pathogens. Plant Physiology and Biochemistry 38:157-163.

Gao L, Wang Y, Li Z, Zhang H, Ye J, Li G (2016). Gene expression changes during the Gummosis development of peach shoots in response to *Lasiodiplodia theobromae* infection using RNA-Seq. Frontiers in Physiology 7:170.

Gao WQ, Lu LH, Srivastava AK, Wu QS, Kuča K (2020). Effects of mycorrhizae on physiological responses and relevant gene expression of peach affected by replant disease. Agronomy 10:186.

He JD, Chi GG, Zou YN, Shu B, Wu QS, Srivastava AK, Kuča K (2020). Contribution of glomalin-related soil proteins to soil organic carbon in trifoliate orange. Applied Soil Ecology 154:103592.

He JD, Dong T, Wu HH, Zou YN, Wu QS, Kuča K (2019). Mycorrhizas induce diverse responses of root *TIP* aquaporin gene expression to drought stress in trifoliate orange. Scientia Horticulturae 243:64-69.

Hu N, Tu XR, Li KT, Ding H, Li H, Zhang HW, Tu GQ, Huang L (2017). Changes in protein content and chitinase and β-1,3-glucanase activities of rice with blast resistance induced by Ag-antibiotic 702. Plant Diseases and Pests 8:33-36.

Kaur N, Gupta AK (2005). Signal transduction pathways under abiotic stress in plants. Current Science 88:1771-1780.

Kawagoe Y, Shiraishi S, Kondo H, Yamamoto S, Aoki Y, Suzuki S (2015). Cyclic lipopetide iturin a structure-dependently induces defense response in Arabidopsis plants by activating SA and JA signaling pathways. Biochemical and Biophysical Research Communications 460:1015-1020.

Lambais MR, Mehdy MC (2010). Spatial distribution of chitinases and β-1,3-glucanase transcripts in bean arbuscular mycorrhizal roots under low and high soil phosphate conditions. New Phytologist 140:33-42.

Li Z, Wang YT, Gao L, Wang F, Ye JL, Li GH (2014). Biochemical changes and defense responses during the development of peach gummosis caused by *Lasiodiplodia theobromae*. European Journal of Plant Pathology 138:195-207.

Liu F, Xiong-Chang OU, Wei JG, Zhan RL, Chang JM (2017). Interaction mechanism between mango and Fusarium mangiferae on transcriptomes. Acta Phytopathologica Sinica 47:224-233.

Ozgonen H, Akgul DS, Erkilic A (2010). The effects of arbuscular mycorrhizal fungi on yield and stem rot caused by *Sclerotium rolfsii* Sace. in peanut. African Journal of Agricultural Research 5:128-132.

Slezack S, Dumas-Gaudot E, Rosendahl S, Kjoller R, Paynot M, Negrel J, Gianinazzi S (1999). Endoproteolytic activities in pea roots inoculated with the arbuscular mycorrhizal fungus *Glomus mosseae* and/or *Aphanomyces euteiches* in relation to bioprotection. New Phytologist 142:517-529.

Tian L, Wu QS, Kuča K, Rahman MH (2018). Responses of four citrus plants to *Phytophthora*-induced root rot. Sains Malaysiana 47:1693-1700.

Ueda H, Kugimiya S, Tabata J, Kitamoto H, Mitsuhara I (2019). Accumulation of salicylic acid in tomato plant under biological stress affects oviposition preference of bemisia tabaci. Journal of Plant Interactions 14:73-78.

Vangelisti A, Natali L, Bernardi R, Sbrana C, Turrini A, Hassani-Pak K ... Giordani T (2018). Transcriptome changes induced by arbuscular mycorrhizal fungi in sunflower (*Helianthus annuus* L.) roots. Scientific Reports 8:4.

Ward JA, Weber CA (2012). Comparative RNA-Seq for the investigation of resistance to *Phytophthora* root rot in the red raspberry 'Latham'. Acta Horticulturae 946:67-72.

Wu QS, He JD, Srivastava AK, Zou YN, Kuča K (2019). Mycorrhizas enhance drought tolerance of citrus by altering root fatty acid compositions and their saturation levels. Tree Physiology 39:1149-1158.

Xie MM, Zhang YC, Liu LP, Zou YN, Wu QS, Kuča K (2019). Mycorrhiza regulates signal substance levels and pathogen defense gene expression to resist citrus canker. Notulae Botanicae Horti Agrobotanici Cluj-Napoca 47:1161-1167.

Xu ML, Korban SS (2002). A cluster of four receptor-like genes resides in the vf locus that confers resistances to apple scab disease. Genetics 162:1995-2006.

Yap YK, Kodama Y, Waller F, Chung KM, Ueda H, Nakamura K, ... Sano H (2005). Activation of a novel transcription factor through phosphorylation by WIPK, a wound-induced mitogen-activated protein kinase in tobacco plants. Plant Physiology 139: 127-137.

Zhang F, Zou YN, Wu QS, Kuča K (2020). Arbuscular mycorrhizas modulate root polyamine metabolism to enhance drought tolerance of trifoliate orange. Environmental and Experimental Botany 171:103962.

Zhang YC, Zou YN, Liu LP, Wu QS (2019). Common mycorrhizal networks activate salicylic acid defense responses of trifoliate orange (*Poncirus trifoliata*). Journal of Integrative Plant Biology 61:1099-1111.